Critical Role of Gravity in Filters

A. D. Araújo,[1] J. S. Andrade, Jr.,[1] and H. J. Herrmann[1,2]
[1]*Departamento de Física, Universidade Federal do Ceará, 60451-970 Fortaleza, Ceará, Brazil*
[2]*IfB, HIF E12, ETH Hönggerberg, CH-8093 Zürich, Switzerland*
(Received 9 February 2006; published 26 September 2006)

The efficiency of filters depends crucially on the mass of the particles one wants to capture. Using analytical and numerical calculations we reveal a very rich scenario of scaling laws relating this efficiency to particle size and density and the velocity and viscosity of the carrying fluid. These are combined in the dimensionless, so-called Stokes number St. In the case of horizontal flow or neutrally buoyant particles, we find a critical number St_c below which no particles are trapped; i.e., the filter does not work. Above St_c the capture efficiency increases like the square root of $(\mathrm{St} - \mathrm{St}_c)$. Under the action of gravity, the threshold abruptly vanishes and capture occurs at any Stokes number increasing linearly in St. We discovered further scaling laws in the penetration profile and as function of the porosity of the filter.

DOI: 10.1103/PhysRevLett.97.138001 PACS numbers: 81.05.Rm, 05.40.−a, 83.10.Pp

In many areas of application as for instance chemical or environmental engineering or medicine, air, and water purification or segregation via filtration play a crucial role [1–3]. In particular, we will focus here on deep bed filtration where the particles in suspension are much smaller than the pores of the filter which they penetrate until being captured at various depths. For non-Brownian particles, at least four capture mechanisms can be distinguished, namely, the geometrical, the chemical, the gravitational, and the hydrodynamical one [1]. Detailed laboratory experiments were conducted some years ago by Ghidaglia *et al.* [4] evidencing a sharp transition in particle capture as a function of the dimensionless ratio of particle to pore diameter characterized by the divergence of the penetration depth.

In this Letter we will focus on the inertial effects in capture which constitute an important mechanism in most practical cases and, despite much effort, are quantitatively not yet understood, as reviewed in Ref. [5]. The effect of inertia on the suspended particles can be quantified by the dimensionless *Stokes number*,

$$\mathrm{St} \equiv V d_p^2 \rho_p / 18 \ell \mu, \tag{1}$$

where d_p and ρ_p are the diameter and density of the particle, respectively, ℓ is a characteristic length of the pores, μ is the viscosity, and V is the velocity of the fluid. Inertial capture by fixed bodies has already been described since 1940 by Taylor and proven to happen for inviscid fluids above a critical Stokes number [6]. This phenomenon has been studied on fixed, periodic arrays of rectangles and cylinders [7] without a more detailed discussion about the nature of an eventual transition.

Let us start by considering an infinite ordered filter composed of a periodic arrangement of fixed circular obstacles (e.g., cylinders). For instance, this type of model has been frequently used to describe the porous geometry of fibrous filters [8]. This system can then be completely described by a single square cell of unitary size and porosity $\epsilon \equiv (1 - \pi D^2/4)$, where D is the actual diameter of the obstacle, as shown in Fig. 1. Assuming Stokesian flow through the void space of this cell and that $\mathbf{u} = 0$ at the boundary, the governing equation for the stream function ψ is given by $\nabla^4 \psi = 0$. An analytical solution $\psi(x, y)$ for this linear biharmonic equation has been given by Marshall *et al.* [8]. We use this solution to obtain the velocity flow field $\mathbf{u}(x, y)$, which is nonuniform, and to study the transport of pointlike particles numerically. As a first approximation, we assume that the influx of suspended particles is so small that (i) the fluid phase is not affected by changes in the particle volume fraction and that (ii) particle-particle interactions are negligible. Moreover, we also consider that the movement of the particles does not transfer momentum to the flow field [9]. Finally, if we assume that the drag force and gravity are the only relevant forces acting on the particles, their trajectories can be calculated by integration of Newton's equation [10]:

$$\frac{d\mathbf{u}_p^*}{dt^*} = \frac{(\mathbf{u}^* - \mathbf{u}_p^*)}{\mathrm{St}} + F_g \frac{\mathbf{g}}{|\mathbf{g}|}, \tag{2}$$

where $F_g \equiv (\rho_p - \rho)\ell|\mathbf{g}|/(V^2\rho_p)$ is a dimensionless parameter, $\mathbf{g}$ is gravity pointing in the positive x direction, t^*

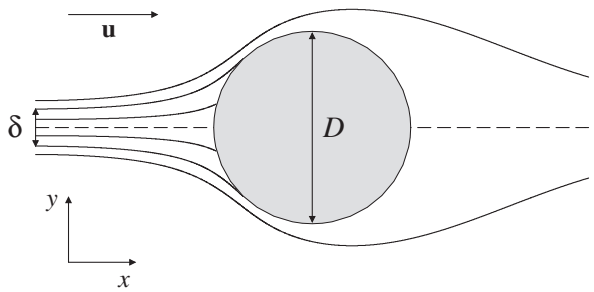

FIG. 1. Particle trajectories when released from different positions at the inlet of the periodic filter cell. The thick solid lines separated by a distance δ at the releasing point correspond to the trajectories that limit the trapping zone in the flow.

is a dimensionless time, and $\mathbf{u}_p^*$ and $\mathbf{u}^*$ are the dimensionless velocities of the particle and the fluid, respectively.

We show in Fig. 1 some trajectories calculated for particles released in the flow for St = 0.25. Once a particle touches the obstacle, it gets trapped. Our objective here is to search for the release position y_0 at the inlet of the unit cell ($x_0 = 0$) and above the horizontal axis (dashed line in Fig. 1), below which the particle is always captured and above which the particle can always escape from the system. Here we assume that the y component of the particle velocity at the inlet is equal to zero, while the x component is set to be equal to the fluid velocity at this location. As depicted in Fig. 1, the particle capture efficiency can be quantitatively defined as $\delta \equiv 2y_0$. In the limiting case St $\rightarrow \infty$, since the particles move ballistically towards the obstacle, the particle efficiency reaches its maximum, $\delta = D$. For St $\rightarrow 0$, on the other hand, the efficiency is smallest, $\delta = 0$. In this last situation, the particles can be considered as tracers that exactly follow the streamlines of the flow, avoiding trapping.

In Fig. 2 the normalized capture efficiency δ/D is shown as a function of the Stokes number for different values of gravity. Interestingly, only for the zero gravity case does the capture efficiency vanish at a finite Stokes number St_c. For any finite value of g, no matter how small, we find a finite efficiency for positive Stokes numbers. Gravity therefore drives the system to a new fixed point with vanishing critical Stokes number.

Next we analyze the critical behavior. In Fig. 3, we show the log-log plot of the variation of δ/D with the rescaled Stokes number in the presence of gravity for three different porosities. In all cases, the variable δ increases linearly with St to subsequently reach a crossover at $\mathrm{St}_\times$, and finally approach its upper limit ($\delta = D$). The results of our simulations also show that $\mathrm{St}_\times \sim (\epsilon - \epsilon_{\min})$, where $\epsilon_{\min}$ corresponds to the minimum porosity below which the distance between inlet and obstacle is too small for a massive particle to deviate from the obstacle. We confirm the validity of this rescaling approach through the collapse of all data as shown in Fig. 3.

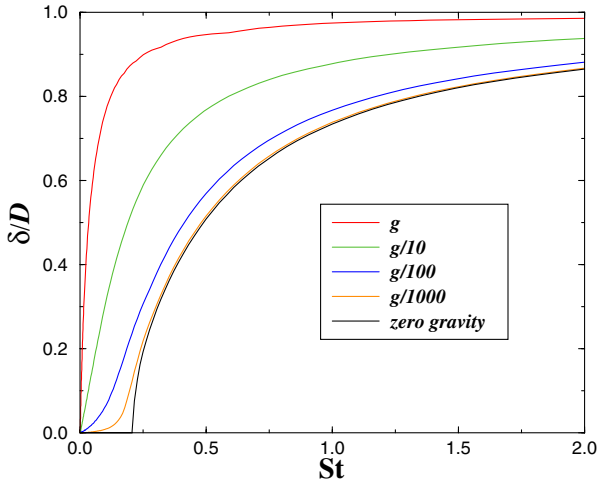

FIG. 2 (color online). Normalized capture efficiency δ as function of the Stokes number St for different values of gravity. For reference, $F_g = 16$ in Eq. (2) corresponds to a value that is compatible with the experiments of Ref. [4] when subjected to the gravity on Earth.

The capture behavior becomes significantly different in the absence of gravity, as shown in the inset of Fig. 3. The efficiency δ remains equal to zero up to a certain critical Stokes number, St_c, that corresponds to the maximum value of St below which particles cannot be captured, regardless of the position y_0 at which they have been released. This is in fact an intricate consequence of the shape of the flow lines as obtained in Marshall's solution [8]. Although controversial [7], some hints for such a finite critical point can be found in previous studies, where potential as well as viscous flow conditions had been considered [11]. Right above St_c, the variation of δ can be described in terms of a power law,

$$\delta \sim (\mathrm{St} - \mathrm{St}_c)^\alpha, \tag{3}$$

with an exponent $\alpha \approx 0.5$. Our results show that, while the exponent α is practically independent of the porosity for $\epsilon > 0.8$, the critical Stokes number decreases with ϵ, and therefore with the distance from the obstacle where the particle is released (see Fig. 3). To our knowledge, the nature of this singularity behavior, which resembles a second order transition, has never been reported before.

Filters are typically disordered. Therefore we adopt now a random pore space geometry that is often used to describe porous media [12]. As shown in Fig. 4, it consists of nonoverlapping circular obstacles of diameter D, separated

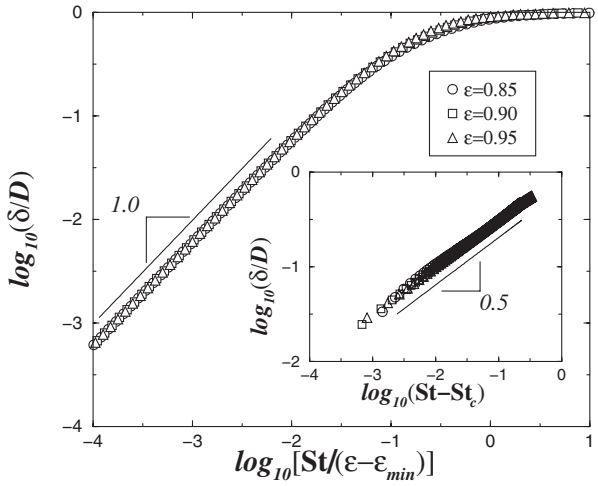

FIG. 3. Log-log plot of the dependence of the capture efficiency δ on the rescaled Stokes number $\mathrm{St}/(\epsilon - \epsilon_{\min})$ for a periodic filter in the presence of gravity. Same parameters as in Fig. 2. The inset shows that the behavior of the system without gravity can be characterized by $\delta \sim (\mathrm{St} - \mathrm{St}_c)^\alpha$, with $\alpha \approx 0.5$ and $\mathrm{St}_c = 0.2679 \pm 0.0001$, 0.2096 ± 0.0001, and 0.1641 ± 0.0001, for $\epsilon = 0.85$, 0.9, and 0.95, respectively.

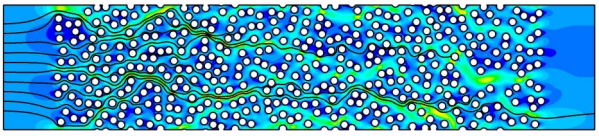

FIG. 4 (color online). Velocity magnitude for a typical realization of a pore space ($\epsilon = 0.7$) subjected to low Reynolds conditions. Fluid is pushed from left to right. The colors ranging from blue to yellow (dark to light grey) correspond to low and high velocity magnitudes, respectively. Also shown are typical trajectories of particles. Gravity points in the positive x direction, and the Stokes number is St $= 0.01$.

by a distance larger than $D/10$, that are randomly allocated in a two-dimensional channel of width h, until a prescribed void fraction ϵ is reached. For compatibility between the periodic and disordered descriptions, we take the characteristic pore size to be $\ell \equiv D/20$ (i.e., half of the minimum distance between any two obstacles of the disordered system). Periodic boundary conditions are applied in the y direction. We use the same geometrical and physicochemical parameters of the experimental set described in Ref. [4].

The fluid mechanics in the porous space is based on the assumptions of a continuum, Newtonian, and incompressible fluid flowing under steady state conditions. Thus, the local velocity and pressure fields of the fluid, $\mathbf{u}$ and p, follow the Navier-Stokes and continuity equations. We consider nonslip boundary conditions along the entire solid-fluid interface. In addition, a uniform velocity profile, $u_x(0, y) = V$ and $u_y(0, y) = 0$, is imposed at the inlet of the channel. The Reynolds number is defined as $\mathrm{Re} \equiv \rho V h/\mu$, where ρ is the density of the fluid. For simplicity, we restrict our study to the laminar viscous regime, i.e., the case where the Reynolds number is sufficiently low ($\mathrm{Re} < 1$).

We obtain the numerical solution of the Navier-Stokes and continuity equations through discretization by means of the control volume finite-difference technique [13]. Considering the complex geometries involved, we build an unstructured mesh of triangular grid elements based on a Delaunay network. For a porosity $\epsilon = 0.6$ we need approximately 10^6 cells to generate satisfactory results.

The local velocity magnitude for a filter of porosity $\epsilon = 0.7$ can be seen in Fig. 4. The transport of momentum through the complex geometry generates typical preferential channels [14]. Once the velocity and pressure fields are obtained for the flow, we proceed with the calculation of particle transport. As before, we assume that the only relevant forces acting on the particles are drag and gravity [15] and calculate the trajectories of the particles through numerical integration of the equations of motion. In order to account for spatial fluctuations of the velocity field, we adopt here the empirical relations proposed by Morsi and Alexander [16], where the local drag is calculated as a function of the local Reynolds number.

We also see in Fig. 4 typical trajectories of particles that have been released from different positions at the inlet of the filter for St $= 0.01$. For a fixed value of St, we consider up to 1000 particles to determine (i) whether these particles get trapped and (ii) the precise position where their capture takes place. From these positions, we plot in the inset of Fig. 5 the profiles of the fraction of noncaptured particles ϕ against the distance x from the inlet. In the limiting case of a very dilute system ($\epsilon \approx 1$) with particles being transported in the ballistic regime ($\mathrm{St} \to \infty$), it is easy to show that $\phi(x) = \exp(-x/\lambda)$, with a penetration length given by $\lambda = \pi D/4(1 - \epsilon)$. For low and moderate values of St, the behavior of $\phi(x)$ is still exponential, but λ now being a function of the Stokes number. We postulate that for any combination of ϵ and St the previous result can be generalized to the following "ansatz":

$$\lambda = \pi D^2/4(1 - \epsilon)\delta, \tag{4}$$

the length δ being the capture efficiency analogously defined as for the periodic filter. As shown in Fig. 5, the penetration length follows a power law $\lambda \sim (\mathrm{St})^{-\alpha}$, with a scaling exponent $\alpha \approx 1$ that is, within the numerical error bars, the same for all values of porosity investigated. Simulations performed for different realizations of the disordered filter resulted in the same exponent. This value is also consistent with the exponent found before for the periodic case with gravity.

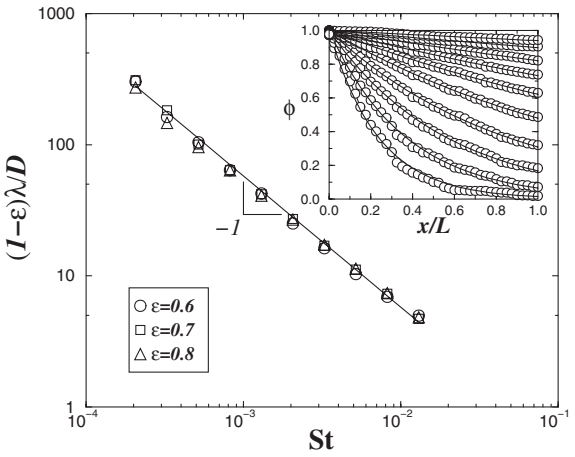

FIG. 5. Log-log plot showing the dependence of the rescaled penetration length $(1 - \epsilon)\lambda/D$ on the Stokes number St for three different porosity values. The solid line corresponds to the best fit to the data of the scaling function $(1 - \epsilon)\lambda/D = \beta \mathrm{St}^{-\alpha}$ with the prefactor $\beta \approx 0.058$ and the exponent $\alpha = 1.00 \pm 0.02$. The inset shows the profiles of ϕ against x corresponding to a porosity $\epsilon = 0.7$ and different values of the Stokes number. From top to bottom, $\mathrm{St} = 2.06 \times 10^{-4}$, 3.26×10^{-4}, 5.18×10^{-4}, 8.2×10^{-4}, 1.3×10^{-3}, 2.06×10^{-3}, 3.26×10^{-3}, 5.18×10^{-3}, 8.2×10^{-3}, and 1.3×10^{-2}. The solid lines are the best fits to the different data sets following $\phi = \exp(-x/\lambda)$, with $\lambda = \lambda(\epsilon, \mathrm{St})$.

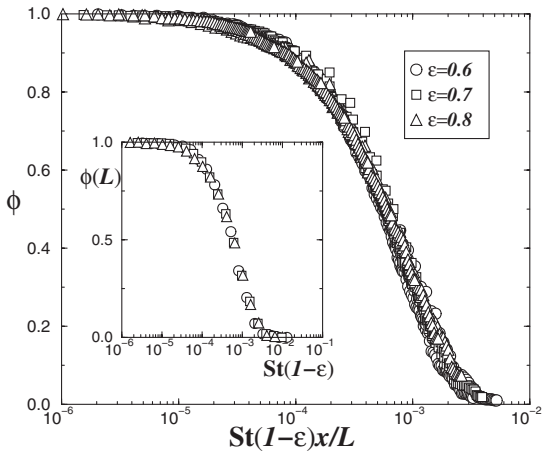

FIG. 6. Log-linear plot showing the global data collapse of the number fraction of particles $\phi(x)$ versus the rescaled distance $\mathrm{St}(1-\epsilon)x/L$. The inset is also a semilog plot showing the effect of inertia on the overall fraction $\phi(L)$ for three different values of porosities.

The data collapse obtained for different values of ϵ as seen in Fig. 5 suggests a relation

$$\frac{\lambda}{D} = \frac{\beta}{\mathrm{St}(1-\epsilon)}, \tag{5}$$

where $\beta \approx 0.058$, which for all practical purposes is a constant for the porous geometry and particle capture studied here. Indeed, as shown in Fig. 6, the data collapse of all profiles of ϕ in terms of the rescaled variable $\mathrm{St}(1-\epsilon)x/L$ provides strong evidence that, under conditions of viscous flow and drag transport, Eq. (5) should remain valid for any value of ϵ and St. A similar argument can also lead to the data collapse of the overall fraction $\phi(L)$ as seen in the inset of Fig. 6.

Summarizing, we have studied the capture of particles in periodic and random filters. In the absence of gravity there exists a finite critical Stokes number below which particles never get trapped. Furthermore, we found that the transition between nontrapping and trapping right above the critical point follows power-law behavior, with a scaling exponent $\alpha \approx 0.5$. Including the action of gravity we show that (i) the nontrapping regime is suppressed (i.e., $\mathrm{St}_c = 0$) and (ii) the scaling exponent changes to $\alpha \approx 1$. In the future, we intend to investigate simultaneous multiple particle release and the possibility of nontrapping at first contact. It would be interesting to experimentally verify the existence of a finite critical Stokes number when gravity is canceled by using either a horizontal setup or neutrally buoyant particles.

We thank Josué Mendes Filho and André Moreira for discussions and acknowledge CNPq, CAPES, FUNCAP, FINEP, and the Max-Planck prize for financial support.

[1] C. Tien, *Granular Filtration of Aerosols and Hydrosols* (Butterworths, Boston, 1989).
[2] M. Sahimi and A. O. Imdakm, Phys. Rev. Lett. **66**, 1169 (1991).
[3] S. Redner and S. Datta, Phys. Rev. Lett. **84**, 6018 (2000).
[4] C. Ghidaglia, L. de Arcangelis, J. Hinch, and E. Guazzelli, Phys. Rev. E **53**, R3028 (1996); Phys. Fluids **8**, 6 (1996).
[5] D. L. Koch and R. J. Hill, Annu. Rev. Fluid Mech. **33**, 619 (2001).
[6] D. E. Rosner and P. Tandon, Chem. Eng. Sci. **50**, 3409 (1995).
[7] A. G. Konstandopoulos, M. J. Labowsky, and D. E. Rosner, J. Aerosol Sci. **24**, 471 (1993); M. Kostoglou and A. G. Konstandopoulos, J. Aerosol Sci. **31**, 427 (2000).
[8] H. Marshall, M. Sahraoui, and M. Kaviany, Phys. Fluids **6**, 507 (1994).
[9] We also investigated both the effects of simultaneous movement of particles and hydrodynamical coupling between particle motion and fluid flow. Each particle in this calculation represents in fact a stream of several grains. Our results show that the effect of this hydrodynamical interaction is to generally *reduce* the value of the releasing distance δ from the symmetry line. If the system is sufficiently diluted, this effect becomes negligible. In the specific case of a Stokes number $\mathrm{St} = 3 \times 10^{-5}$ and a ratio $q_p/q_f = 10^{-4}$, where q_p is the particle flow rate at the stream and q_f is the fluid flow rate through the periodic cell, the value of δ is only 5% smaller than its counterpart calculated for the uncoupled condition. Let us also point out again that although our Stokes numbers [Eq. (1)] imply that the particles have finite diameter, the simulations treat the particles as pointlike.
[10] A fifth order Runge-Kutta subroutine has been used to numerically solve the equation of motion Eq. (2). A relative precision of 10^{-6} in the trajectory coordinates and local velocities of the particle is obtained and shown to be sufficient to determine the critical Stokes number with a relative precision of 0.01%.
[11] L. M. Levin, Izdatel'stvo Academii Nauk SSSR Report No. FTD-HT-23-1593-67, 1961 (English translation); N. A. Fuchs, *The Mechanics of Aerosols* (Pergamon, New York, 1964); D. B. Ingham, L. T. Hildyard, and M. L. Hildyard, J. Aerosol Sci. **21**, 935 (1990); D. Lesnic, L. Elliott, and D. B. Ingham, Mathematika **41**, 277 (1994); C. G. Phillips and S. R. Kaye, J. Aerosol Sci. **30**, 709 (1999).
[12] S. Torquato, *Random Heterogeneous Materials: Microstructure and Macroscopic Properties* (Springer-Verlag, New York, 2001).
[13] S. V. Patankar, *Numerical Heat Transfer and Fluid Flow* (Hemisphere, Washington, DC, 1980); the FLUENT (trademark of FLUENT, Inc.) fluid dynamics analysis package has been used in this study.
[14] J. S. Andrade, Jr., U. M. S. Costa, M. P. Almeida, H. A. Makse, and H. E. Stanley, Phys. Rev. Lett. **82**, 5249 (1999).
[15] J. K. Comer, C. Kleinstreuer, and C. S. Kim, J. Fluid Mech. **435**, 55 (2001).
[16] S. A. Morsi and A. J. Alexander, J. Fluid Mech. **55**, 193 (1972).